Available online at www.sciencedirect.com
ScienceDirect
Geochimica et Cosmochimica Acta 74 (2010) 6276–6286
Geochimica et Cosmochimica Acta
www.elsevier.com/locate/gca

Variations of $^{17}O/^{16}O$ and $^{18}O/^{16}O$ in meteoric waters

Boaz Luz *, Eugeni Barkan

The Institute of Earth Sciences, The Hebrew University of Jerusalem, Jerusalem 91904, Israel

Received 25 March 2010; accepted in revised form 11 August 2010; available online 18 August 2010

Abstract

The variations of $\delta^{17}O$ and $\delta^{18}O$ in recent meteoric waters and in ice cores have proven to be an important tool for investigating the present and past hydrologic cycle. In order to close significant information gaps in the present distribution of $\delta^{17}O$ and $\delta^{18}O$ of meteoric water, we have run precise measurements, with respect to VSMOW, on samples distributed globally from low to high latitudes. Based on the new and existing data, we present the Global Meteoric Water Line (GMWL) for $\delta^{17}O$ and $\delta^{18}O$ as:

$$\ln(\delta^{17}O + 1) = 0.528 \ln(\delta^{18}O + 1) + 0.000033 \quad (R^2 = 0.99999)$$

In addition to meteoric water, we carried out the first measurements of seawater from the Pacific and Atlantic oceans with respect to VSMOW. The obtained results show that the slope of the trend line $\ln(\delta^{17}O + 1)$ vs. $\ln(\delta^{18}O + 1)$ of seawater samples is 0.528, the same as for meteoric water, but the regression intercept is −5 per meg. Thus, the positive intercept in the GMWL indicates an excess of ^{17}O in meteoric waters with respect to the ocean. An excess (or depletion) of ^{17}O in water is defined as:

$$^{17}O\text{-excess} = \ln(\delta^{17}O + 1) - 0.528(\delta^{18}O + 1)$$

Most meteoric water samples have positive ^{17}O-excess of varying magnitudes with an average of 37 per meg with respect to VSMOW. We explain how these positive values originate from evaporation of sea water into marine air, which is undersaturated in water vapor, and how subsequent increase of ^{17}O-excess occurs when atmospheric vapor condenses to form liquid and solid precipitation. We also clarify the effect of excessive evaporation on ^{17}O-excess. Finally, based on the new results on ^{17}O-excess of seawater we recalculated the relationship of $\delta^{17}O$ vs. $\delta^{18}O$ in vapor diffusion in air as $^{18}\alpha_{diff} = 1.0096$.

1. INTRODUCTION

In studies on natural variations in isotopic concentrations, water isotope ratios ($HD^{16}O/H_2{}^{16}O$ and $H_2{}^{18}O/H_2{}^{16}O$) have played a key role in understanding the hydrologic cycle (e.g. Craig, 1961; Dansgaard, 1964). In general, the ratios D/H or $^{18}O/^{16}O$ vary mainly due to phase changes from vapor to liquid or ice and vice versa. The ratios of hydrogen isotopes (expressed as δD) and oxygen isotopes (expressed as $\delta^{18}O$) are linearly correlated, and the trend of variations characterizes the Global Meteoric Water Line (GMWL) where $\delta D = 8\delta^{18}O + 10$ (Craig, 1961). For the most part, the positive intercept in this regression originates from the difference in isotopic fractionation effects of water-vapor equilibrium and of vapor diffusion in air (e.g. review of Gat, 1996). Deviations from a line with slope of 8 and zero intercept indicate an excess (or depletion) of deuterium and are calculated for a water sample as: d-excess $= \delta D - 8\delta^{18}O$.

The seminal papers of Merlivat and Jouzel (1979) and Jouzel and Merlivat (1984) formulated the basis for the interpretation of d-excess in ice cores and other meteoric waters in terms of relative humidity at the source oceanic regions. Later on, Johnsen et al. (1989) pointed out the importance of temperature in the source oceanic regions in controlling the magnitude of d-excess, and this was followed by the application of d-excess in ice cores as an

* Corresponding author. Tel.: +972 2 6585224; fax: +972 2 5662581.
E-mail address: boaz.luz@huji.ac.il (B. Luz).

0016-7037/$ - see front matter © 2010 Elsevier Ltd. All rights reserved.
doi:10.1016/j.gca.2010.08.016

indicator of oceanic temperature variations in glacial and interglacial times (e.g. Vimeux et al., 1999). Notably, Petit et al. (1991) observed a large increase in d-excess of surface Antarctic snow between coastal and inland sites. In explaining this trend, it was necessary to account for kinetic effects controlled by ice condensation from supersaturated vapor.

The focal point of the present paper is to demonstrate how relationships between $H_2{}^{17}O/H_2{}^{16}O$ (or $\delta^{17}O$) and $H_2{}^{18}O/H_2{}^{16}O$ (or $\delta^{18}O$), similar to those between δD and $\delta^{18}O$, yield unique information on evaporation conditions above the ocean. The importance of the $\delta^{17}O$–$\delta^{18}O$ tool is that it is far less sensitive to temperature effects than the δD–$\delta^{18}O$ pair.

Luz and Barkan (2000) were the first to demonstrate that the relationship between $\delta^{17}O$ and $\delta^{18}O$ is different in evaporation than in equilibrium controlled processes affecting meteoric waters. Additional indication for the role of equilibrium and diffusion effects in evaporation came from a global budget of factors affecting $\delta^{17}O$ and $\delta^{18}O$ of atmospheric oxygen (Angert et al., 2003). These findings led to the suggestion that $\delta^{17}O$ and $\delta^{18}O$ in meteoric waters may yield unique information on past relative humidity independently of temperature isotope effects that complicate the interpretation of d-excess (Angert et al., 2004). It was clear, however, that realization of the potential of $\delta^{17}O$ and $\delta^{18}O$ in hydrology required the development of a high precision analytical method for oxygen isotope analyses of water. Such method, based on fluorination of water with CoF_3, was developed by us and used to measure the fractionations in liquid–vapor equilibrium and in the diffusion of water vapor in air (Barkan and Luz, 2005, 2007). We have recently run the first $\delta^{17}O$ and $\delta^{18}O$ measurements of oceanic vapor (Uemura et al., 2010). The data (for the southern parts of the Indian and Pacific Oceans) show clear evidence of positive ^{17}O-excess in marine vapor, its negative correlation with relative humidity, but no sensitivity to wind speed. These results confirmed the importance of oxygen isotope fractionation of both equilibrium and diffusion in oceanic evaporation. In addition to the study of recent vapor, we have measured $\delta^{17}O$ and $\delta^{18}O$ in the Vostok ice core, and demonstrated an increase in ^{17}O-excess over glacial–interglacial transitions (Landais et al., 2008). The change in ^{17}O-excess was interpreted as an indication for higher relative humidity over the source oceanic region in glacial times.

From Meijer and Li (1998) we know that the slope of the trend line of $\ln(\delta^{17}O + 1)$ vs. $\ln(\delta^{18}O + 1)$ is 0.528. However, the precision of the measurements in that study was not high enough for hydrological applications. Our group confirmed the 0.528 slope in high precision measurements of surface Antarctic snow (Landais et al., 2008), but the information on low latitudes remained very sparse. Furthermore, in the above studies the isotopic ratios were reported with respect to the VSMOW standard, assuming that this standard represents the average $\delta^{17}O$ and $\delta^{18}O$ of ocean water. This, however, has never been confirmed experimentally.

The goal of the present paper is to close information gaps and to give an integrated picture showing the significance of variations in $\delta^{17}O$ and $\delta^{18}O$ of natural waters. With this purpose, we analyzed samples of seawater and meteoric waters distributed globally. In addition, we ran an open pan evaporation experiment in order to understand how the oxygen isotope composition of meteoric water may be modified by excessive evaporation. Together with previous data generated in our lab and published elsewhere, we give an integrated view on the distributions of $\delta^{17}O$ and $\delta^{18}O$ in precipitation and the factors controlling their variations.

2. EXPERIMENTAL

2.1. Isotopic analyses

The analytical method for determination of the oxygen isotopic ratios in water is detailed in Barkan and Luz (2005). In short, 2 μl of water are converted by fluorination into O_2 gas using CoF_3 reagent. The produced O_2 is transferred into a stainless steel holding tube on a collection manifold immersed in liquid helium. At the end of 10 sample processing, the manifold is separated from the preparation line and the holding tubes are warmed up to room temperature. Then the manifold is connected to a Thermo-Finnigan Delta^{plus} isotope-ratio mass spectrometer (Thermo Scientific, Bremen, Germany). The ratio $^{18}O/^{16}O$ is measured in dual inlet mode by multi-collector mass spectrometry. Each mass spectrometric measurement consists of three separate runs during which the ratio of sample to reference is determined 30 times. The pressures of the sample and reference gases are balanced before each of the three runs. The reported δ-values are averages of three runs with respect to VSMOW. The mass spectrometer errors (standard error of the mean ($n = 90$) multiplied by Student's t-factor for a 95% confidence limits) in $\delta^{18}O$ and $\delta^{17}O$ are 0.004 and 0.008‰, respectively.

In a previous study (Barkan and Luz, 2005) we verified that our mass spectrometers are linear. We repeatedly measured the value of SLAP vs. VSMOW and it remained within the experimental error −55.11‰ (measured on O_2 gas as reported in Barkan and Luz, 2005). Our result is about 0.4‰ different than the consensus SLAP vs. VSMOW value of −55.5‰, which is based on measurements of CO_2 gas (Gonfiantini, 1978). We emphasize that we did not apply any stretching to the measured $\delta^{18}O$ values in order to make them fit the consensus value. The reason for this is that in preliminary experimental work we found that there were small but systematic differences in the measured $\delta^{18}O$ values between pairs of CO_2 and pairs of O_2 gases that were prepared to have identical isotopic composition. This probably indicates some unknown mass spectrometric artifacts. Because more experimental work is needed in order to clarify this phenomenon, we decided not to apply any correction at this stage.

2.2. Isotopic fractionations and notations

In the standard notation, δ is given by Eq. (1) as:

$$\delta = \frac{R_{sample}}{R_{ref}} - 1 \quad (1)$$

where R stands for the ratio between water containing heavy isotopes ($H_2{}^{17}O$, $H_2{}^{18}O$ or HDO) and $H_2{}^{16}O$ (note that for convenience we omit the factor of 10^3 but the δ^*O results are reported in ‰).

It has been shown (e.g. Miller, 2002; Luz and Barkan, 2005) that when dealing with high precision ratios in multiple isotope systems, a modified δ, hereafter designated δ′, should be preferred. This modified δ is defined as:

$$\delta' = \ln(\delta + 1) = \ln\left(\frac{R_{sample}}{R_{ref}}\right) \quad (2)$$

In the stable isotope literature, fractionation factors (α′s) are presented such that they are greater or smaller than unity depending on how they are defined. In the present paper α′s are given such that they are always greater than 1. For example, for equilibrium fractionation between vapor (V) and liquid (W) the fractionation factor is defined as: $\alpha_{eq} = R_W/R_V$ (and not R_V/R_W), where R_W and R_V are the ratios between heavy and light isotope species of water ($H_2{}^{17}O/H_2{}^{16}O$ or $H_2{}^{18}O/H_2{}^{16}O$) in liquid and vapor phase, respectively.

Since equilibrium and diffusion processes play a key role in the hydrologic cycle, in our previous studies (Barkan and Luz, 2005, 2007) we have experimentally determined the relationships among fractionations of the three oxygen isotope species of water (expressed as $\theta = \ln(^{17}\alpha)/\ln(^{18}\alpha)$, Luz and Barkan, 2005) for both vapor–liquid equilibrium (θ_{eq}) and due to diffusive transport of water vapor in air (θ_{diff}). The results were: $\theta_{eq} = 0.529 \pm 0.001$ and $\theta_{diff} = 0.518 \pm 0.0002$.

Based on measured $\delta^{17}O$ and $\delta^{18}O$ values of meteoric water from different climate regions, Barkan and Luz (2007) defined a new parameter, ^{17}O-excess as:

$$^{17}O\text{-excess} = \delta'^{17}O - 0.528\delta'^{18}O \quad (3)$$

Because the magnitudes of the ^{17}O-excess are very small, they are multiplied by 10^6.

3. RESULTS

3.1. Seawater

The results of seawater measurements are given in Table 1 and Fig. 1. The relationships of $\delta'^{18}O$ to geographic location and depth are in agreement with the general pattern known since the seminal study of Craig and Gordon (1965). The deep samples from both the Pacific and Atlantic Oceans are close to VSMOW. Somewhat larger variations are found in shallower samples with higher values in the Atlantic than in the Pacific. The maximum ^{18}O enrichments are found in samples from the E. Mediterranean and the N. Red Sea (2.2‰ and 2.4‰, respectively), where evaporation rates are high. Despite the small range of variations, $\delta'^{17}O$ and $\delta'^{18}O$ are highly correlated ($R^2 = 0.99985$) with a regression slope of 0.528 ± 0.001. The regression intercept is -0.005 ± 0.001‰, in excellent agreement with the average ^{17}O-excess of −5 per meg. We thus conclude that VSMOW is a well suited standard for representing the triple isotopic composition of seawater.

3.2. Meteoric waters

The results for meteoric waters are given in Table 2. These results are plotted in Fig. 2 together with data on Antarctic snow (Landais et al., 2008) and on the GISP and SLAP standards (Barkan and Luz, 2005). Based on these data, the Global Meteoric Water Line (GMWL) for oxygen isotopes is defined as:

$$\delta'^{17}O = 0.528\delta'^{18}O + 0.000033 \quad (4)$$

The most striking features in Fig. 2 are the tight correlation between $\delta'^{17}O$ and $\delta'^{18}O$ ($R^2 = 0.99999$), the regression slope of 0.528 ± 0.0001 and the positive regression intercept

Table 1
Locations and isotopic composition of seawater samples (all values are given versus VSMOW). Atlantic Ocean (1–18), Pacific Ocean (19–36), E. Mediterranean (37) and northern Red Sea (38). Note that due to the very high importance of these data, all the samples were run in triplicate, and the given values are averages with precision (absolute difference from the average) 0.02–0.03‰ for both $\delta^{17}O$ and $\delta^{18}O$ and 4 per meg for ^{17}O-excess.

#	Latitude (°N)	Longitude (°E)	Depth (m)	$\delta^{17}O$ (‰)	$\delta^{18}O$ (‰)	^{17}O-excess (per meg)
1	−31.9667	16.9667	2	0.428	0.839	−15
2	−32.8500	14.6000	2	0.310	0.596	−5
3	−30.7167	4.6833	2	0.330	0.628	−2
4	−28.7500	5.7500	2	0.371	0.710	−4
5	−25.4000	−22.9833	2	0.543	1.044	−8
6	−22.4667	−25.0000	5390	−0.130	−0.236	−5
7	−22.4667	−25.0000	2000	0.063	0.134	−8
8	−22.4667	−25.0000	750	−0.041	−0.067	−6
9	−20.2000	−25.0000	2	0.486	0.932	−6
10	−12.5167	−25.0000	2	0.419	0.807	−7
11	−4.4333	−25.0000	2	0.435	0.840	−8
12	1.1833	−25.5667	2	0.275	0.529	−4
13	12.8167	−31.1667	2	0.281	0.545	−7
14	19.0667	−34.2667	2	0.598	1.142	−5
15	31.3833	−42.1333	2	0.641	1.217	−1
16	33.9167	−46.0833	2	0.660	1.252	−1
17	34.9167	−42.8833	1000	0.231	0.459	−11
18	41.1500	−26.3833	2	0.551	1.045	−1
19	0.0000	155.0000	10	0.058	0.117	−4
20	0.0000	155.0000	500	0.043	0.092	−6
21	0.0000	155.0000	1000	−0.038	−0.059	−7
22	0.0000	155.0000	1600	0.020	0.051	−7
23	0.0000	155.0000	2000	−0.027	−0.033	−10
24	0.0000	155.0000	2400	−0.057	−0.102	−3
25	0.0000	155.0000	2542	−0.047	−0.070	−10
26	35.0000	139.0000	10	0.178	0.343	−3
27	35.0000	139.0000	500	−0.048	−0.069	−12
28	35.0000	139.0000	1000	−0.047	−0.083	−3
29	47.0000	160.0000	500	−0.225	−0.415	−6
30	47.0000	160.0000	1000	−0.159	−0.289	−6
31	47.0000	160.0000	1600	−0.165	−0.315	1
32	47.0000	160.0000	2000	−0.065	−0.130	4
33	47.0000	160.0000	2500	−0.064	−0.126	3
34	47.0000	160.0000	3000	−0.049	−0.095	1
35	47.0000	160.0000	4000	−0.029	−0.062	4
36	47.0000	160.0000	5196	−0.032	−0.057	−2
37	32.0833	34.7667	0	1.140	2.172	−6
38	29.5000	34.9167	0	1.276	2.416	1

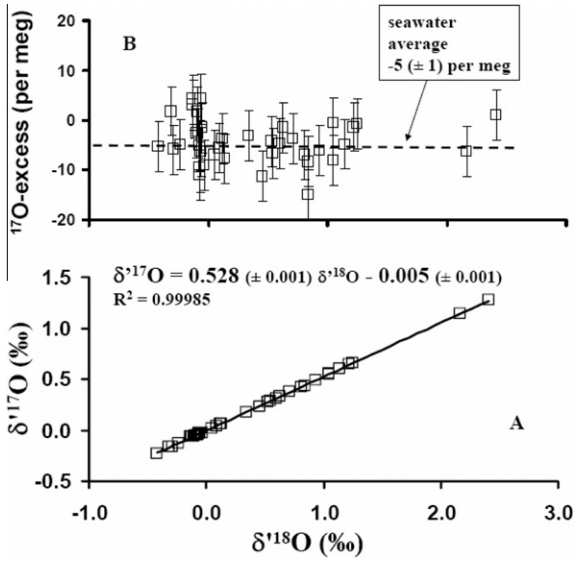

Fig. 1. Plots showing the isotopic composition of seawater: (A) $\delta'^{17}O$ vs. $\delta'^{18}O$, the error bars are smaller than the size of the symbols; (B) ^{17}O-excess vs. $\delta'^{18}O$. The data are given in Table 1.

($0.033 \pm 0.003‰$). Importantly, the calculated regression slope (0.528) is not sensitive to changes in the data base, and as long it is calculated for a large set of globally distributed samples it will remain the same. For example, a slope of the same magnitude was derived by Meijer and Li (1998) and Barkan and Luz (2007) for entirely different data sets.

As shown in Fig. 2, most meteoric waters have positive ^{17}O-excess, and there is no trend in its values against latitude. The average excess of ^{17}O in meteoric waters with respect to VSMOW is 37 per meg, but the excess with respect to the ocean is slightly greater (42 per meg) because as shown above, the average ^{17}O-excess of ocean waters with respect to VSMOW is −5 per meg. The difference between ^{17}O-excess of vapor and seawater should be taken into account in model studies.

As can be seen, there are local variations in ^{17}O-excess of meteoric waters. These may reflect differences in ^{17}O-excess of vapor in the source oceanic regions, excessive evaporation of meteoric waters or kinetic effects in polar precipitation. We discuss these variations below.

3.3. Open pan experiment

The experiment was carried out in the lab. Air relative humidity and temperature were about 80% and 22 °C. It was started by placing distilled water in an open Petri dish, and water was subsequently lost by evaporation. Evaporative loss was measured by weighing the dish. The results of the open pan experiment are given in Table 3 and Fig. 3. The trend of $\delta'^{18}O$ with respect to the remaining fraction is very similar to that observed by Craig et al. (1963) with relatively steep rise at the beginning of the experiment and attainment of steady state towards the end. As the remaining fraction went low and $\delta'^{18}O$ increased, ^{17}O-excess decreased.

4. DISCUSSION

4.1. The $\delta'^{17}O$ vs. $\delta'^{18}O$ slope in meteoric waters

To a large extent, the observed trend of $\delta'^{17}O$ vs. $\delta'^{18}O$ in meteoric waters can be explained if it is assumed that condensation of vapor to liquid due to air cooling occurs in isotopic equilibrium. For a simple example we consider liquid precipitation and Rayleigh distillation of vapor that occurs with constant ${}^{*}\alpha_{eq}$ ("*" stands for 17 or 18). Starting from atmospheric vapor with a given $\delta'^{*}O_o$, the $\delta'^{*}O$ of the remaining fraction (f) of vapor after rainout is:

$$\delta'^{*}O - \delta'^{*}O_o = ({}^{*}\alpha_{eq} - 1)\ln(f) \quad (5)$$

and the slope (γ) of meteoric water, which is derived from the vapor, is:

$$\gamma = \frac{(\delta'^{17}O - \delta'^{17}O_o)}{(\delta'^{18}O - \delta'^{18}O_o)} = \frac{({}^{17}\alpha_{eq} - 1)}{({}^{18}\alpha_{eq} - 1)} \quad (6)$$

Over the temperature range 0–30 °C, $^{18}\alpha_{eq}$ varies from 1.01182 to 1.00894 (Horita and Wesolowski, 1994) and correspondingly $^{17}\alpha_{eq}$ ($=^{18}\alpha_{eq}^{0.529}$) varies from 1.00623 to 1.00472. In this case, $(^{17}\alpha_{eq} - 1)/(^{18}\alpha_{eq} - 1)$ remains nearly constant and about 0.528 (0.5275–0.5279). At sub-freezing temperatures the calculated slope is somewhat smaller than the observed one, and we will explain this difference in the section on polar precipitation.

We note, that the reason for the small difference between the slope of the equilibrium line (0.529) and the slope of the GMWL (0.528) is that in the first case it is defined as $\theta = \ln(^{17}\alpha_{eq}/^{18}\alpha_{eq})$, while in the second as $\gamma = (^{17}\alpha_{eq} - 1)/(^{18}\alpha_{eq} - 1)$ (for details see Luz and Barkan, 2005).

4.2. The origin of ^{17}O-excess in meteoric waters

As mentioned above, almost all meteoric waters have an ^{17}O-excess with respect to ocean water. For the most part, it can be explained by steady state evaporation from the ocean following the model of Craig and Gordon (1965).

The origin of the positive ^{17}O-excess of marine vapor is shown schematically in Fig. 4. According to the Craig–Gordon concept, vapor in the immediate vicinity of a water surface has relative humidity of 100% and is in isotopic equilibrium with the water. Because the slope of the equilibrium line (0.529) is greater than that of the GMWL (0.528), ^{17}O-excess of equilibrium vapor is slightly negative (−9 and −11 per meg at 5 and 25 °C, respectively).

Continuing with the Craig–Gordon concept, vapor from the equilibrium layer is transported by diffusion into the free air above along a line with $\theta_{diff} = 0.518$. Because the diffusive slope is smaller than the slope of the GMWL (0.528), diffusion tends to increase ^{17}O-excess of marine vapor. The extent of this increase depends on the gradient of vapor concentration between the saturated layer near the water surface and the free air above (see Fig. 4). It will increase when this gradient becomes stronger (lower relative humidity in free air) and vice versa.

Notably, a similar explanation applies to the origin of deuterium excess in marine air (e.g. Gat, 1996). However, whereas the effect of sea surface temperature is negligible

Table 2
Locations, dates and isotopic composition of meteoric waters (all values are given versus VSMOW, see Table 1 for precision).

#	Country	Location	Date	$\delta^{17}O$ (‰)	$\delta^{18}O$ (‰)	^{17}O-excess (per meg)
1	Austria	Dunabe river (Vienna)	1-Apr-07	−5.184	−9.829	18
2	Canada	Boneyard Cave BC	5-Feb-05	−4.621	−8.817	44
3	Canada	Boneyard Cave BC	5-Jul-05	−5.029	−9.570	36
4	Canada	Rats Nest Cave AB	5-Jul-05	−9.251	−17.544	51
5	Canada	Con Cave BC-1	5-Jan-05	−5.279	−10.117	76
6	Canada	Con Cave BC-2	5-Jul-05	−5.675	−10.849	68
7	China	Yalong river, Yang Shou	1-Oct-07	−3.081	−5.925	52
8	Montenegro	Sedlo Pass, snow	1-Jun-06	−2.865	−5.397	−12
9	Croatia	Lake Kozjak (Plitvice)	1-Jul-06	−4.965	−9.415	17
10	Germany	Ahr River (Altenahr)	1-Aug-07	−3.972	−7.561	27
11	Germany	Rhein River (Koeln)	1-Aug-07	−4.873	−9.239	16
12	Germany	Small stream (near Bacharach)	1-Aug-07	−4.126	−7.843	23
13	Germany	Neckar river (Heidelberg)	1-Aug-07	−4.164	−7.911	21
14	India	New Delhi (average rain)	2005–2007	−1.306	−2.513	22
15	India	Ahamedabad (average rain)	2008 (June–Sept.)	−2.351	−4.486	20
16	India	Kozhikod (average rain)	2001–2004	−1.709	−3.272	20
17	India	Nal Sarovar	Feb 2007	2.177	4.158	−16
18	Indonesia	Borneo, rain	5-Mar-05	−2.926	−5.626	49
19	Indonesia	Borneo, rain	5-Jun-05	−3.573	−6.857	54
20	Indonesia	Borneo, rain	5-Aug-05	−3.568	−6.847	53
21	Indonesia	Borneo, rain	5-Nov-05	−4.687	−8.969	59
22	Israel	Jerusalem (average rain)	2006–2007	−2.458	−4.717	35
23	Israel	Jerusalem (Telem Spring)	1-Feb-08	−2.962	−5.699	51
24	Israel	Jerusalem tap water	1-Aug-08	−2.193	−4.206	30
25	Israel	Snir River	1-Jul-08	−3.388	−6.510	55
26	Israel	Dan River	1-Jul-08	−3.778	−7.243	53
27	Israel	Jordan River	1-Jul-08	−3.308	−6.323	36
28	Israel	Lake Kinneret	1-Jul-08	−0.008	−0.060	24
29	Israel	Lake Kinneret	1-Jul-07	−0.369	−0.739	21
30	New Zealand	Pukaki River	1-Feb-08	−5.068	−9.665	47
31	New Zealand	Waiau River	1-Feb-08	−4.226	−8.094	56
32	Russia	Lake Onega, 0 m	1-May-08	−5.749	−10.936	40
33	Russia	Lake Onega, 37 m	1-May-08	−5.237	−9.951	30
34	Russia	Lake Ladoga	1-May-08	−5.003	−9.529	40
35	Russia	Lake Baikal	1-Jul-03	−8.412	−15.913	22
36	Russia	Neva River (St. Petersburg)	1-May-08	−4.993	−9.511	40
37	Switzerland	Lake Davos	1-Aug-02	−6.679	−12.655	23
38	Switzerland	Lake Zurich	1-Aug-02	−5.445	−10.337	26
39	Switzerland	Lake Lucern	1-Sep-99	−6.692	−12.681	24
40	Turkey	Duden Falls (near Antalya)	1-Dec-07	−3.712	−7.078	32
41	USA	Marengo Cave IN	5-Jan-06	−3.308	−6.342	46
42	USA	Marengo Cave IN	5-Jul-05	−3.345	−6.416	48
43	USA	Howe Caverns NY	5-Jan-05	−4.396	−8.369	32
44	USA	Howe Caverns NY	5-Jul-05	−4.492	−8.553	33
45	USA	New Bruswick NJ (pond)	1-Jun-07	−2.635	−5.016	17
46	USA	Hudson River (Piermont NY)	1-Aug-07	−3.543	−6.728	15
47	USA	Winnipesaukee River (Tilton NH)	1-Aug-07	−3.401	−6.476	24
48	Uzbekistan	Chirchiq River (near Charvak)	1-May-08	−6.368	−12.091	35
49	Antarctica	Dome F		−31.059	−58.009	1
50	Canada	Edmonton, snow	4-Dec-09	−13.735	−25.927	40
51	Canada	Edmonton, snow	23-Jan-10	−10.747	−20.329	39
52	France	Seine River (Triel sur Seine)	Oct-09	−3.172	−6.040	22

in the case of ^{17}O-excess, it is significant in the case of deuterium excess. The reason for this is that θ_{eq} is identical at all temperatures in the case of the three oxygen isotopes, but in contrast, the ratio of the D/H equilibrium isotope effect to that of $^{18}O/^{16}O$ becomes greater as temperature decreases. Therefore, ^{17}O-excess is a direct proxy for humidity of marine air while the deuterium excess proxy for humidity must be corrected for temperature effects.

Following the model of Craig and Gordon (1965), Barkan and Luz (2007) explained the ^{17}O-excess of marine vapor in terms of humidity and the diffusion fractionation factor $^{18}\alpha_{diff}$. Below we present an adaptation of the Craig and

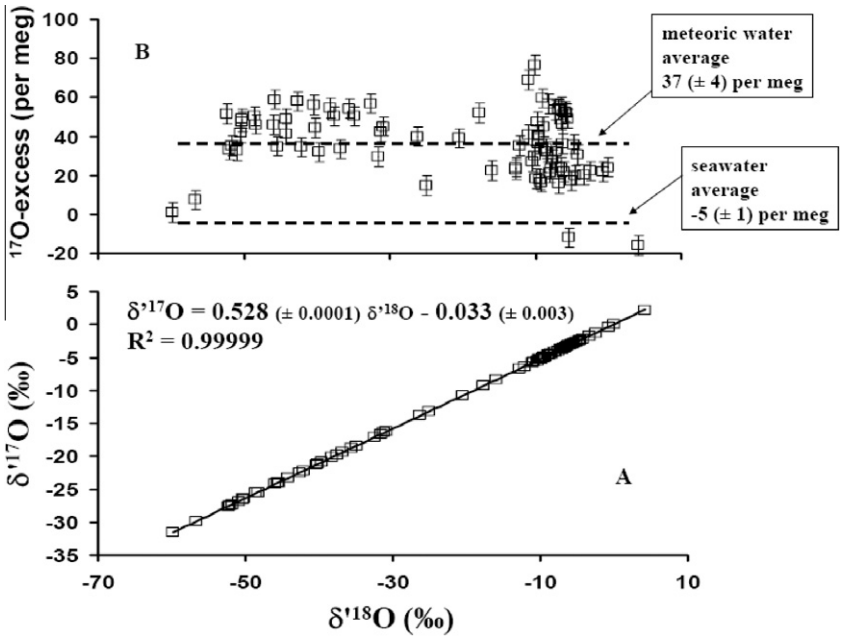

Fig. 2. Plots showing the isotopic composition of meteoric water: (A) $\delta'^{17}O$ vs. $\delta'^{18}O$, the error bars are smaller than the size of the symbols; (B) ^{17}O-excess vs. $\delta'^{18}O$ (the data points are from Table 2, Landais et al. (2008) and Barkan and Luz (2005)).

Table 3
Data of the open pan experiment.

Time (h)	Remaining fraction	$\delta^{18}O$ (‰)	$\delta^{17}O$ (‰)	^{17}O-excess (per meg)
0.0	1.00	−4.879	−2.541	38
55.0	0.65	4.937	2.578	−26
74.5	0.55	7.686	4.005	−46
97.5	0.40	8.505	4.419	−62
118.0	0.30	8.460	4.391	−67

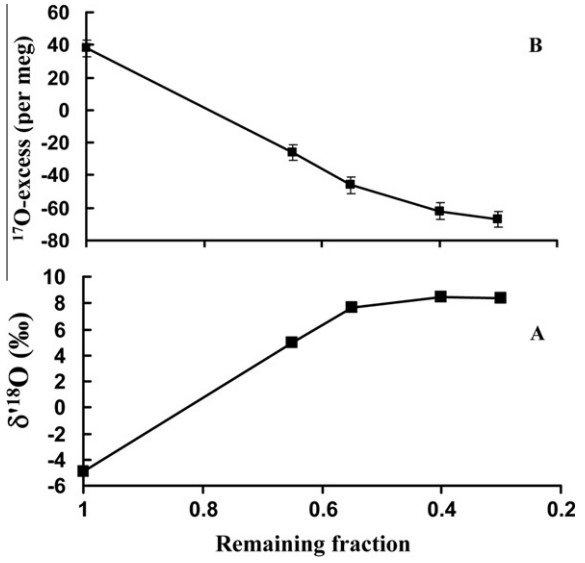

Fig. 3. Plots of $\delta'^{18}O$ and ^{17}O-excess vs. remaining water fraction in the open pan experiment. The error bars for $\delta'^{18}O$ (A) are smaller than the size of the symbols.

Gordon (1965) model, casting isotopic variations in terms of ratios and fractionation factors rather than δ's and isotope effects (ε's) used by Craig and Gordon and several other papers that follow their model. This treatment is better suited for the explanation of ^{17}O-excess.

The isotopic fractionation factor between an evaporating flux (E) and a liquid water surface (W) is defined as: $\alpha_{evap} = R_W/R_E$, where R_W and R_E are the isotopic ratios ($H_2{}^{17}O/H_2{}^{16}O$ or $H_2{}^{18}O/H_2{}^{16}O$) of the liquid surface and the vapor flux, respectively. α_{evap} can be expressed in a general form as (Barkan and Luz, 2007):

$$\alpha_{evap} = R_W/R_E = \frac{\alpha_{diff}\alpha_{eq}(1-h)}{1-\alpha_{eq}h(R_A/R_W)} \quad (7)$$

where R_A is the isotopic ratio of air moisture, α_{eq} and α_{diff} are the equilibrium and the diffusive fractionation factors, respectively, and h is relative air humidity.

Eq. (7), with only slight differences, was originally obtained in three ways: from diffusion theory (Ehhalt and Knott, 1965), from kinetic theory (Criss, 1999) and based on a steady state evaporation model (Cappa et al., 2003). Importantly, Enhalt and Knott derived an equation similar to Eq. (7) by *a priory* assuming that α_{diff} depends only on diffusivities of the various isotopic species in air, and for turbulent conditions they obtained $\alpha_{diff} = (D_{light}/D_{heavy})^{1/2}$. Yet, α_{diff} also depends on the thickness of the boundary layer, temperature etc. (see for details Merlivat and Jouzel, 1979; Gat et al., 2001; Cappa et al., 2003; Horita et al., 2008). This raises the question whether Eq. (7) is suitable for explaining natural conditions. However, in the other two derivations (Criss and Cappa et al.) it was not necessary to explicitly define how α_{diff} is related to molecular or turbulent diffusion. Therefore, Eq. (7) is general and is applicable for modeling

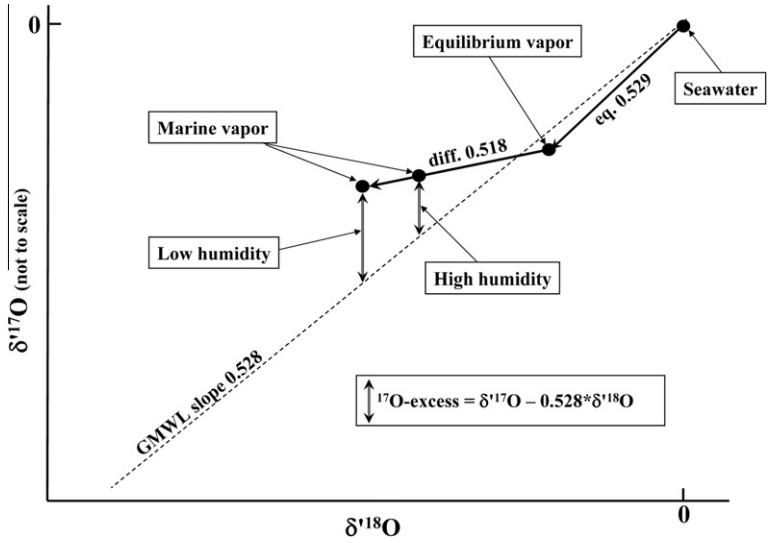

Fig. 4. Schematic presentation of evaporation from the ocean showing the origin of ^{17}O-excess in marine vapor (see text for explanation).

evaporation processes in experimental as well as natural conditions.

For the most part, the isotopic composition of marine vapor can be explained by taking into account only vapor–liquid equilibrium and vapor diffusion in air (Craig et al., 1963). To explore the tendency of the influence of changing climatic conditions on this isotopic composition, we used the so called "closure assumption" (Merlivat and Jouzel, 1979). According to the closure assumption the only source of vapor in the boundary layer is from surface evaporation. In this case, the isotopic ratio of marine vapor equals to that of the net evaporating flux, $R_A = R_E$. Using this condition, natural log transformation and rearrangement of Eq. (7) we obtain:

$$\ln({}^{*}R_E/{}^{*}R_W) = -\ln({}^{*}\alpha_{eq}({}^{*}\alpha_{diff}(1-h_n)+h_n)) \quad (8)$$

The asterisk stands for either 17 or 18. Importantly, we use h_n instead of ordinary relative humidity (h), where h_n is the ratio of vapor concentration of free air to saturated concentration at the temperature and salinity of the sea surface (see Gat, 1984).

The term on the left of Eq. (8) is δ' of atmospheric vapor (R_E) with respect to seawater (R_W), and then, based on its definition (Eq. (3)), the ^{17}O-excess of this vapor is expressed as:

$$\begin{aligned} {}^{17}\text{O-excess} = &-\ln({}^{18}\alpha_{eq}^{0.529}({}^{18}\alpha_{diff}^{0.518}(1-h_n)+h_n)) \\ &+0.528\cdot\ln({}^{18}\alpha_{eq}(\alpha_{diff}(1-h_n)+h_n)). \end{aligned} \quad (9)$$

As discussed in Barkan and Luz (2007), ^{17}O-excess is practically insensitive to sea surface temperature (despite its effect on $^{18}\alpha_{eq}$), but depends on both $^{18}\alpha_{diff}$ and h_n.

Clearly, the closure assumption is a simplification of the natural situation and its validity may be questionable (Jouzel and Koster, 1996; Delmotte et al., 2000). However, our previous study (Uemura et al., 2010) strongly suggests that while mixing of moisture from sources other than direct marine evaporation may have strong effect on δ^{18}O, it does not influence the ^{17}O-excess. Therefore, the simple closure assumption appears to work well in explaining the origin of the ^{17}O-excess in oceanic vapor. Furthermore, Risi et al. (2010) confirmed the above conclusion in a recent modeling study. They showed that while the modeled δ^{18}O and d-excess values may be considerably inaccurate (up to several per mile in the latter), for ^{17}O-excess the situation is much better. The difference between ^{17}O-excess values calculated for vapor over tropical and subtropical oceans using the closure assumption and a more sophisticated single-column model (SCM), as well as a mixed cloud isotopic model (MCIM), is only 3 per meg, significantly smaller than our analytical precision (5 per meg).

In Fig. 5 we show the relationship of ^{17}O-excess of marine vapor over the south Indian Ocean and Southern Ocean with respect to seawater versus h_n (the measured data are

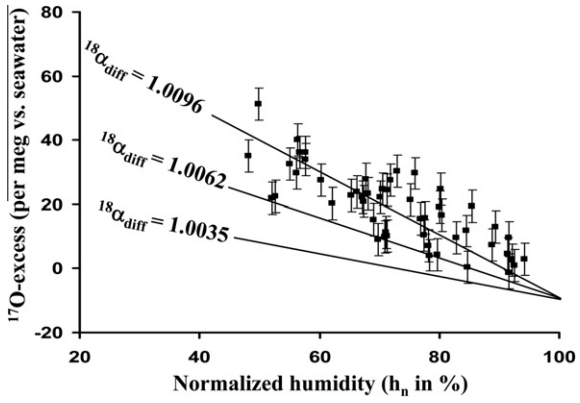

Fig. 5. The relationship between ^{17}O-excess and normalized relative humidity of marine air. The ^{17}O-excess and h_n data are from Uemura et al. (2010). We added 5 per meg to each original ^{17}O-excess data point in order to correct for the difference between seawater and VSMOW. The best fit to the data is a model line (based on Eq. (9)) with $^{18}\alpha_{diff}$ of 1.0096. For comparison we also show lines calculated with $^{18}\alpha_{diff}$ of 1.0062 and 1.0035 for smooth and rough regimes as in Merlivat and Jouzel (1979).

from Uemura et al., 2010). The slope of the best fit line (−1.04 per meg/‰) is in very good agreement with Risi et al. (2010), who calculated, using their SCM, the sensitivity of ^{17}O-excess of low-altitude vapor to h_n as −1.0 per meg/‰, which was also similar to that predicted by the closure assumption. Moreover, Risi et al., based on their modeling considerations, showed that ^{17}O-excess of marine vapor is affected mainly by the relative humidity at the surface, in full agreement with Eq. (9).

In summary, from the above consideration it follows that the closure assumption describes correctly the link between relative humidity and ^{17}O-excess of marine vapor. Therefore, Eq. (9) despite its simplicity is suitable for reliable estimation of $^{18}\alpha_{diff}$ from measurements of isotopic ratios in marine vapor.

In the present study $^{18}\alpha_{diff}$ was estimated from the best fit line (Fig. 5) as 1.0096 ± 0.0018. The obtained value of $^{18}\alpha_{dif}$ is greater than the one determined by Uemura et al. The only reason for this is that in the present calculations we corrected the original data points (that were given with respect to VSMOW) for the difference between seawater and VSMOW. The given value is at present the best available estimate that should be used in future modeling studies.

The magnitude of ^{17}O-excess in marine air versus seawater ranges from slightly negative values at high humidity to above 40 per meg in samples taken at the lowest humidity end (Fig. 5). The average ^{17}O-excess of marine air with respect to seawater is about 20 per meg, much smaller than the average ^{17}O-excess of meteoric water with respect to seawater ($42 = 37 + 5$ per meg). In part, this difference indicates that the major flux of marine moisture, that eventually forms precipitation, is derived from warmer parts of the ocean where relative humidity is lower (and ^{17}O-excess of vapor is higher) than over colder ocean surface (Peixoto and Oort, 1996). However, it is unlikely that most of the precipitation would form from vapor originating only from regions of lowest relative humidity. Thus, there should be an additional mechanism for increasing ^{17}O-excess.

In Fig. 6 we explain in a schematic way how further increase of ^{17}O-excess should occur. When vapor condenses in isotopic equilibrium to liquid or solid, the trajectory from vapor to the condensed phase has a slope of 0.529, which is greater than 0.528 of the GMWL. Precipitation, therefore, is formed with higher ^{17}O-excess than its source vapor. For example, for precipitation forming at −10 and −40 °C the ^{17}O-excess increases by 17 and 23 per meg, respectively. The significance of this increase can be demonstrated as follows. The measured ^{17}O-excess in polar precipitation is about 38 per meg versus VSMOW (Landais et al., 2008). Correcting for the difference of 5 per meg between seawater and VSMOW, ^{17}O-excess of polar precipitation with respect to seawater is about 43 per meg. Assuming 23 per meg is representative for the increase in polar precipitation, the corresponding ^{17}O-excess of its source marine vapor is about 20 per meg. This, in turn, corresponds to normalized relative humidity of about 72% (Fig. 5). We note, however, that for better estimations from ice core records it will be necessary to use relevant climatic information for the site of each ice core.

Of course, as condensation increases the ^{17}O-excess of the formed liquid or solid, the ^{17}O-excess of the remaining vapor must go low, and thus slightly reducing the effect described above. However, due to the non-linearity of the ^{17}O-excess to $\delta^{18}O$ relationships, the evolution lines (in $\delta'^{17}O$ vs. $\delta'^{18}O$ plots) of both vapor and liquid forming during equilibrium precipitation are slightly curved. And as a result, this causes an increase in ^{17}O-excess of precipitation as $\delta^{18}O$ decreases in the distillation process (see curve A on Fig. 7). This point is discussed further in Section 4.3 in the context of precipitation in Antarctica.

Finally, it has been suggested (Miller, 2008 and references therein) that the excess of ^{17}O in Antarctic snow with respect to ocean water might be the result of lowering of the tropopause in winter and introduction of anomalously ^{17}O-enriched stratospheric-vapor. Evidently, the lack of an increase of ^{17}O-excess with latitude shows that this cannot be a significant source of high ^{17}O enrichment in Antarctic

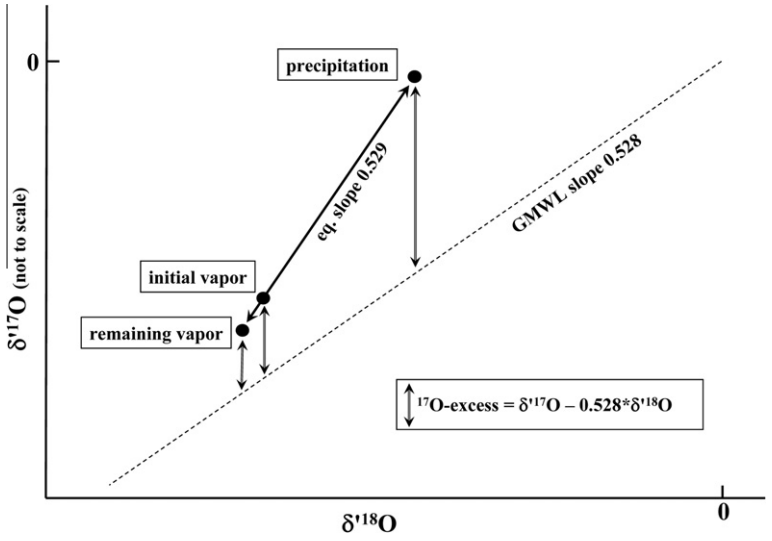

Fig. 6. A schematic presentation showing the increase of ^{17}O-excess in the transition from vapor to precipitation.

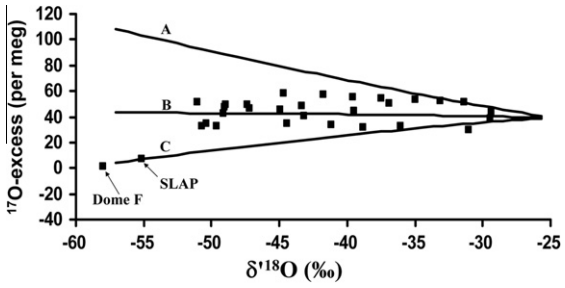

Fig. 7. A plot showing ^{17}O-excess vs. δ'^{18}O in Antarctic precipitation and simulated curves with different kinetic effects. (A) No kinetic effect ($q = 0$); (B) low kinetic effect ($q = 0.0010$) that fits well the data of Landais et al. (2008); (C) stronger kinetic effect ($q = 0.0015$) that fits well the data of SLAP and Dome F.

snow. In fact, in certain polar samples the ^{17}O-excess is unusually low (SLAP and Dome F in Figs. 2 and 7). Below we explain how such lowering is possible by a kinetic effect associated with condensation of vapor to ice.

4.3. Variations of ^{17}O-excess in polar precipitation

As explained above, the fractionation between water vapor and condensed phases is temperature dependent. When such condensation occurs in equilibrium, non-linearity of the ^{17}O-excess to δ^{18}O relationships will cause a calculated evolution line (in δ'^{17}O vs. δ'^{18}O plot) to be slightly curved and its slope to become slightly smaller at low δ^{18}O. Due to this non-linearity, ^{17}O-excess is expected to increase as δ^{18}O decreases by a simple Rayleigh distillation in a cooling air mass. Angert et al. (2004), who first modeled δ^{17}O and δ^{18}O in polar precipitation, assumed that this expected increase in ^{17}O-excess may be compensated for by diffusive isotopic effect which is relevant when vapor condenses to solid ice at low temperature (Jouzel and Merlivat, 1984). With new data presented here and also previous data generated in our lab on Antarctic snow (Barkan and Luz, 2005; Landais et al., 2008), we can test this assumption.

With the above purpose, we use a simple precipitation and fractionation simulation model similar to that of Jouzel and Merlivat (1984). In this, as well as in other such models, atmospheric vapor condenses to form ice due to progressive cooling of air masses. As is well known, in such process heavier isotopes are preferentially removed to ice, and as a result, the remaining vapor becomes depleted in heavy isotopes. This isotopic fractionation is controlled by both solid–vapor equilibrium fractionation (α_{sv}) and kinetic fractionation due to vapor diffusion through air into the precipitation site (α_{kin}). Accordingly, the ratios $H_2{}^{17}O/H_2{}^{16}O$ or $H_2{}^{18}O/H_2{}^{16}O$ in solid (s) and vapor (v) are related as shown in Eq. (10):

$$R_s = R_v(\alpha_{sv}/\alpha_{kin}) \tag{10}$$

Following Jouzel and Merlivat (1984), α_{kin} can be expressed as:

$$\alpha_{kin} = \frac{\alpha_{SV} \cdot \alpha_{diff} \cdot (S-1)+1}{S} \tag{11}$$

where S is supersaturation, which is assumed to be linearly related to cloud temperature (t) such that $S = 1 - q{\cdot}t$, where t is in °C.

In Fig. 7 we show ^{17}O-excess vs. δ^{18}O data of surface snow samples from Antarctica (Landais et al., 2008) and three simulated curves. Curve A is for the case where $q = 0$, and it is clear that it does not fit the observations. A much better fit was obtained with a slight effect of diffusive fractionation (curve B; $q = 0.001$). However, two points fall below this curve (SLAP standard (Barkan and Luz, 2005) and Dome F (Table 2) with ^{17}O-excess of 7 and 1 per meg, respectively). By increasing q to 0.0015 (curve C) we obtained good fit to these two points. This suggests that in certain Antarctic locations the effect of diffusive fractionation is different. We cannot explain why kinetic effects are variable and suggest doing more study on this question in future research.

Regardless of the exact magnitude of the kinetic effect on ^{17}O-excess of Antarctic snow, the simple simulation done here, shows that the kinetic effect must be considered in the assessment of ^{17}O-excess in polar precipitation. We note, however, that improved estimation should be possible by application of more sophisticated models (e.g. mixed cloud isotope models of Ciais and Jouzel, 1994 or Kavanaugh and Cuffey, 2003), and also by additional field observations and experiments at sub-freezing temperatures.

4.4. Lowering of ^{17}O-excess by excessive evaporation

In two sampling sites shown in Fig. 2, values of the ^{17}O-excess are negative (Nal Sarovar, India −16 per meg and Sedlo Pass, Montenegro −12 per meg, Lines 17 and 8 in Table 2). Nal Sarovar is a lake that fills up during the summer monsoon and is subject to intense evaporation in the following months. The sample shown was taken in February, 2007 and we compare it with average monsoon rain from Ahamedabad (Table 2, line 15), assuming the latter represents the isotopic composition of the lake prior to subsequent evaporation. On average, monsoon rains in Ahmedabad have δ^{18}O of −4.49‰ and ^{17}O-excess of 20 per meg. Due to evaporation, water in Nal Sarovar increased in δ^{18}O from −4.49‰ to 4.15‰, and this increase was accompanied by lowering of ^{17}O-excess by 36 per meg. Such lowering is in a good agreement with our experimental data for evaporation from an open pan (Table 3, Fig. 3), which show even stronger lowering of ^{17}O-excess.

We suggest that excessive evaporation applies also to the sample from Sedlo Pass. This sample is snow that remained in June, 2006 from the previous winter. It must have undergone much melting, evaporation and refreezing prior to our sampling. We do not know what its initial isotopic composition was, but suppose that its unusually low ^{17}O-excess also reflects substantial evaporation.

Another example of ^{17}O-excess lowering by evaporation is clearly seen in Lake Kinneret, Israel. Water being fed to the lake originates in tributaries of Jordan River (Dan and Snir Rivers). An increase in δ^{18}O of about 7‰ is observed between the source water in the tributaries and L. Kinneret water, and this enrichment is accompanied by about 30 per meg lowering of the ^{17}O-excess (Table 2, lines 25–29).

The presented results allow us to conclude that while in the case of a very large reservoir, as the ocean, where evaporation does not affect the remaining liquid, the effect of evaporation on small water bodies is large. These changes of ^{17}O-excess must be taken into account in the interpretation of data from paleo-waters, as well as ice core data, unless it can be assured that partial melting and evaporation did not occur after the snow had accumulated.

5. CONCLUSIONS

1. The ^{17}O-excess of seawater with respect to VSMOW is only slightly negative (−5 per meg). Therefore, VSMOW is a well suited standard for representing the ocean in studies involving measurements of ^{17}O-excess. However, in model studies the observed difference should be taken into account.
2. Based on the data set of globally distributed samples of meteoric waters, we define the Global Meteoric Water Line (GMWL) for oxygen isotopes as: $\delta'^{17}O = 0.528\delta'^{18}O + 0.000033$. The positive intercept indicates an excess of ^{17}O in meteoric waters with respect to the ocean.
3. The excess of ^{17}O originates from evaporation of sea water into marine air, which is undersaturated in water vapor, and from the transfer of atmospheric vapor to liquid or solid precipitation.
4. High ^{17}O-excess in meteoric water is indicative of oceanic origin where air relative humidity is low and vice versa. Significant lowering of ^{17}O-excess occurs when a reservoir of meteoric water is subject to excessive evaporation.
5. Based on the new data on ^{17}O-excess of seawater with respect to VSMOW, the relationship of $\delta^{17}O$ vs. $\delta^{18}O$ in vapor diffusion in air is calculated as $^{18}\alpha_{diff} = 1.0096$.

ACKNOWLEDGMENTS

We owe special thanks to two colleagues: Jan Kaiser for sampling seawater from the Atlantic and V.V.S.S. Sarma for samples from the Pacific Ocean. We also thank other colleagues who sent us samples of meteoric waters: Osamu Abe, Tom Chacko, Kim Cobb, Amaelle Landais, Oded Navon, Saikat Sengupta, Henry Schwarcz, Igor Tokarev, and Viacheslav Tikhomirov. James Farquhar, Kazimierz Rozanski, Alexander Van Hook and an anonymous reviewer read the manuscript and made many constructive suggestions. This research was supported by the Israel Science Foundation (Grant No. 181/06).

REFERENCES

Angert A., Rachmilevitch S., Barkan E. and Luz B. (2003) Effects of photorespiration, the cytochrome pathway, and the alternative pathway on the triple isotopic composition of atmospheric O_2. *Global Biogeochem. Cycles* **17**, 1030, doi:10.1029/2002GB001933.

Angert A., Cappa C. D. and DePaolo D. J. (2004) Kinetic ^{17}O effects in the hydrologic cycle: indirect evidence and implications. *Geochim. Cosmochim. Acta* **68**, 3487–3495.

Barkan E. and Luz B. (2005) High precision measurements of $^{17}O/^{16}O$ and $^{18}O/^{16}O$ of O_2 in H_2O. *Rapid Commun. Mass. Spectrom.* **19**, 3737–3742.

Barkan E. and Luz B. (2007) Diffusivity fractionations of $H_2{}^{16}O/H_2{}^{17}O$ and $H_2{}^{16}O/H_2{}^{18}O$ in air and their implications for isotope hydrology. *Rapid Commun. Mass. Spectrom.* **21**, 2999–3005.

Cappa C. D., Hendricks M. B., DePaolo D. J. and Cohen C. (2003) Isotopic fractionation of water during evaporation. *J. Geophys. Res.* **D108**, 4525, doi:10.1029/2003JD003597.

Ciais P. and Jouzel J. (1994) Deuterium and oxygen 18 in precipitation: isotopic model, including mixed cloud processes. *J. Geophys. Res.* **D99**, 16,793–16,803.

Craig H. (1961) Isotopic variations in meteoric waters. *Science* **133**, 1702–1703.

Craig H., Gordon L. I. and Horibe Y. (1963) Isotopic exchange effects in the evaporation of water. *J. Geophys. Res.* **68**, 5079–5087.

Craig H. and Gordon L. I. (1965) *Stable Isotope in Oceanographic Studies and Paleotemperatures*. V. Lischi e Figli, Pisa, p. 122.

Criss R. E. (1999) *Principles of Stable Isotope Distribution*. Oxford University Press, New York, 264p.

Dansgaard W. (1964) Stable isotopes in precipitation. *Tellus* **16**, 436–468.

Delmotte M., Masson V., Jouzel J. and Morgan V. (2000) A seasonal deuterium excess signal at Law Dome, coastal eastern Antarctica: a Southern Ocean signature. *J. Geophys. Res.* **D105**, 7187–7197.

Ehhalt D. and Knott K. (1965) Kinetische Isotopentrennung bei fer Verdampfung von Wasser. *Tellus* **3**, 389–397.

Gat J. R. (1984) The stable isotope composition of Dead Sea waters. *Earth Planet. Sci. Lett.* **71**, 361–376.

Gat J. R. (1996) Oxygen and hydrogen isotopes in the hydrologic cycle. *Annu. Rev. Earth Planet. Sci.* **24**, 225–262.

Gat J. R., Mook W. G. and Meijer H. A. J. (2001) Atmospheric Water. In: *Environmental Isotopes in the Hydrological Cycle*, vol. II. (Ed. W. G. Mook). Technical Documents in Hydrology, No. 39, UNESCO, Paris.

Gonfiantini R. (1978) Standards for stable isotope measurements in natural compounds. *Nature* **271**, 534–536.

Horita J. and Wesolowski D. J. (1994) Liquid-vapor fractionation of oxygen and hydrogen isotopes of water from the freezing to the critical temperature. *Geochim. Cosmochim. Acta* **58**, 3425–3437.

Horita J., Rozanski K. and Cohen S. (2008) Isotope effects in the evaporation of water: a status report of the Craig–Gordon model. *Isot. Environ. Health Stud.* **44**, 23–49.

Johnsen S. J., Dansgaard W. and White J. W. C. (1989) The origin of Arctic precipitation under present and glacial conditions. *Tellus* **41B**, 452–468.

Jouzel J. and Merlivat L. (1984) Deuterium and oxygen 18 in precipitation: modeling of the isotopic effects during snow formation. *J. Geophys. Res.* **D89**, 11749–11757.

Jouzel J. and Koster R. D. (1996) A reconsideration of the initial conditions used for stable water isotope models. *J. Geophys. Res.* **D101**, 22,933–22,938.

Kavanaugh J. L. and Cuffey K. M. (2003) Space and time variation of $\delta^{18}O$ and δD in Antarctic precipitation revised. *Global Biogeochem. Cycles* **17**, 1017, doi:10.1029/2002GB001910.

Landais A., Barkan E. and Luz B. (2008) Record of $\delta^{18}O$ and ^{17}O-excess in ice from Vostok Antarctica during the last 150,000 years. *Geophys. Res. Lett.* **35**, L02709, doi:10.1029/2007GL032096.

Luz B. and Barkan E. (2000) Assessment of oceanic productivity with the triple-isotope composition of dissolved oxygen. *Science* **288**, 2028–2031.

Luz B. and Barkan E. (2005) The isotopic ratios $^{17}O/^{16}O$ and $^{18}O/^{16}O$ in molecular oxygen and their significance in biogeochemistry. *Geochem. Cosmochim. Acta* **69**, 1099–1110.

Meijer H. A. J. and Li W. J. (1998) The use of electrolysis for accurate $\delta^{17}O$ and $\delta^{18}O$ isotope measurements in water. *Isotopes Environ. Health Stud.* **34**, 349–369.

Miller M. F. (2002) Isotopic fractionation and the quantification of ^{17}O anomalies in the oxygen three-isotope system: an appraisal and geochemical significance. *Geochim. Cosmochim. Acta* **66**, 1881–1889.

Miller M. F. (2008) Comment on "Record of $\delta^{18}O$ ^{17}O-excess in ice from Vostok Antarctica during the last 150,000 years" by Amaelle Landais et al.. *Geophys. Res. Lett.* **35**, L23708, doi:10.1029/2008GL034505.

Merlivat L. and Jouzel J. (1979) Global climatic interpretation of the deuterium–oxygen 18 relationship for precipitation. *J. Geophys. Res.* **84**, 5029–5033.

Peixoto J. and Oort A. H. (1996) The climatology of relative humidity in the atmosphere. *J. Clim.* **9**, 3443–3463.

Petit J. R., White J. W. C., Young N. W., Jouzel J. and Korotkevich Y. S. (1991) Deuterium excess in recent Antarctic snow. *J. Geophys. Res.* **96**, 5113–5122.

Risi C., Landais A., Bony S., Jouzel J., Masson-Delmotte V. and Vimeux F. (2010) Understanding the ^{17}O excess glacial–interglacial variations in Vostok precipitation. *J. Geophys. Res.* **115**, D10112, doi:10.1029/2008JD011535.

Uemura R., Barkan E., Abe O. and Luz B. (2010) Triple isotope composition of oxygen in atmospheric water vapor. *Geophys. Res. Lett.* **37**, L04402, doi:10.1029/2009GL041960.

Vimeux F., Masson V., Jouzel J., Stievenard M. and Petit J. R. (1999) Glacial–interglacial changes in ocean surface conditions in the Southern Hemisphere. *Nature* **398**, 410–413.

Associate editor: James Farquhar